



Effect of Fixed Anchor Length on the Bearing Capacity and Failure Mode of Anchor Cables

Liangjun Dai^{1,a}, Tao Cheng^{1,b}, Guojuan Xu^{2,*}

¹Anhui road & bridge engineering Co., Ltd., Hefei, 230031, China

²College of Civil Engineering, Hefei University of Technology, Hefei, 230009, China

^adlj@aceg.com.cn, ^bcgto1983@sina.com,

*2020170701@hfut.edu.cn

Abstract. Bearing capacity of anchor cables are influenced by numerous factors, with the proportion of fixed anchor length playing a critical role in both bearing performance and construction cost. However, previous studies have often overlooked the significance of this parameter. In this paper, numerical simulations are employed to explore the effect of the fixed anchor length proportion on the bearing capacity and failure modes of anchor cables. Simulations were conducted for anchor cables with fixed anchor length ratios of 1, 0.9, 0.85, 0.8, 0.75, 0.7, 0.65, 0.6, 0.55, and 0.5 under identical burial depth conditions. The results reveal that when the fixed anchor length proportion exceeds 0.75, the bearing capacity initially increases and then stabilizes with further increases in the ratio. This trend is consistent with the behavior observed when the ratio is below 0.75. However, the failure patterns differ between the two cases. For fixed anchor length proportions greater than 0.75, the failure pattern manifests as an "inverted cone" extending to the ground surface, whereas for proportions less than 0.75, the failure pattern is "ellipsoidal," without surface extension.

Keywords: proportion of fixed anchor length, bearing capacity, failure mode

1 Introduction

Rock anchoring techniques are widely used in dams, cableways, transmission lines, and bridges [1,2]. In recent years, many researchers have investigated the mechanical behavior of systematic anchors and their installation problems through numerical analysis, similar model tests, and field monitoring, which has greatly improved our understanding of their bearing characteristics [3,4].

Numerous researchers have explored various factors influencing anchoring performance [5,6]. It was observed that as burial depth increased, the damage mode of the anchor cable underwent a transition from rock shear damage to a composite mode comprising upper rock shear damage and lower mortar-rock interface bond damage [7]. Wang et al. (2015) observed through pullout tests of anchors with different diameters and burial depths that the failure mode evolved from interfacial failure to shear failure in the surrounding rock as the diameter of the anchors increased [8]. Su et al. (2021)

found that the maximum shear stress of the anchors occurs at a distance from the anchor head of approximately 25 times the diameter of the anchor. It decreases to zero at a distance of more than 110 times the anchor diameter from the anchor head [9]. Mo-hyeddin et al. (2020) conducted tensile tests on six different thread shapes of anchor cables, revealing a significant relationship between the bearing capacity of the anchor cable and its thread design [10]. Optimization of the installation angle proved to be a more efficacious approach than the augmentation of the surrounding rock strength [11].

The influence of anchor diameter, surrounding rock strength, burial depth, grouting material, and other factors on anchor bearing capacity has been more clearly understood [12-14]. However, the mechanism by which the proportion of anchored sections affects the bearing capacity of anchor rods remains unclear. This study, therefore, aims to investigate the influence of the ratio of fixed anchor length on the bearing capacity of anchor rods under identical conditions of burial depth through the use of numerical simulation.

2 Numerical Simulation

2.1 Model Establishment

A numerical model was developed, where the anchoring interfaces within the rock mass were represented using interface elements, while the contact interfaces responsible for force transfer were modeled with contact elements. The simulations were conducted using interface elements based on the Mohr-Coulomb model. Cable units were utilized for the anchors. The Taoyuan coal mine sandstone in Anhui Province, China, was selected as the rock body, and its mechanical parameters were illustrated in Table 1.

Table 1. Mechanical parameters[14]

Performance parameters	Tensile strength/MPa	Yield strength/MPa	Shear modulus/GPa	Bulk modulus/GPa	Cohesion /MPa	Internal friction angle/°
Surrounding rocks	3.2	0.96	3.3	5.1	4.6	38

2.2 Simulation Scheme

The simulation program was developed according to the anchor design criteria. The anchor depth was set to 5 m, the anchor diameter to 200 mm and the hole diameter to 250 mm. The specific scenarios are given in Table 2.

Table 2. Simulation schemes

proportion of the fixed anchor length	Burial depth/m	Fixed anchor length/m	Free anchor length/m
1	5.0	10.0	10.0
0.9	5.0	8.2	9.1

proportion of the fixed anchor length	Burial depth/m	Fixed anchor length/m	Free anchor length/m
0.85	5.0	7.4	8.7
0.8	5.0	6.7	8.3
0.75	5.0	6.0	8.0
0.7	5.0	5.4	7.7
0.65	5.0	4.8	7.4
0.6	5.0	4.3	7.1
0.55	5.0	3.8	6.9
0.5	5.0	3.3	6.7

3 Results

According to the results shown in Fig. 1, in the initial loading stage, the cables are in the linear elasticity stage and the tensile deformation of the cables increases proportionally to the load, showing good linear elasticity characteristics. As the load increases, the cable enters the yielding stage. At this stage, the cable begins to show plastic deformation. As the load continues to increase, the deformation rate of the rebar accelerates. After continuous loading, the rebar enters the hardening stage. The rate of deformation increases significantly until the anchor fails.

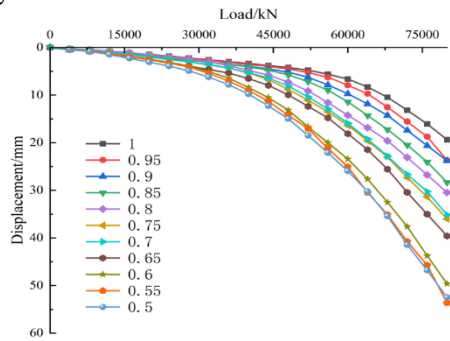


Fig. 1. Load-displacement curve

As shown in Fig. 2, the bearing capacity of the anchor cable shows an overall increasing trend as the proportion of fixed anchor length increases. It can be divided into two stages. Taking 0.75 as the boundary, the proportion of anchored length greater than 0.75 or less than 0.75 is divided into two different stages. The load capacity of the anchor cable with a proportion of fixed anchor length less than 0.75 is less than that of the anchor cable with a proportion of anchorage greater than 0.75. In both stages, the bearing capacity of the anchor cable increases as the proportion of fixed anchor length increases, eventually stabilizing to a certain level. It is not better to have a higher proportion of fixed anchor length.

The failure mode of the anchor cables differs for the two different stages of appeal, as shown in Fig. When the ratio of fixed anchor length is exceeds 0.75, the failure mode

of the anchor cable is an 'inverted cone' rock shear failure extending to the surface, as shown in Fig. 3(a). If the ratio of the anchored section is less than 0.75, it is a closed 'ellipsoidal' rock body local shear damage, as shown in Fig. 3(b). For both types of failure modes, the bearing capacity of the anchor cable increases and then remains unchanged as the anchorage ratio increases. This is because the shear stress increases logarithmically as the proportion of fixed anchor length increases, i.e. the incremental increase in the resistance of the anchor gradually decreases as the proportion of anchored sections increases until it reaches 0.

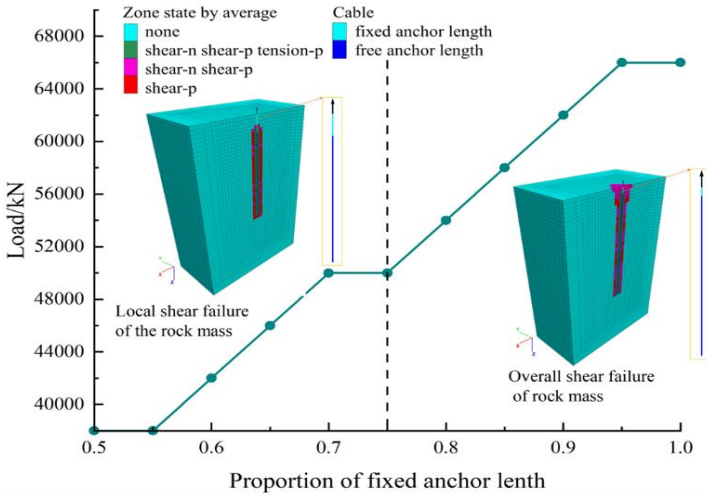


Fig. 2. Relationship between the proportion of the fixed anchor length and the bearing capacity

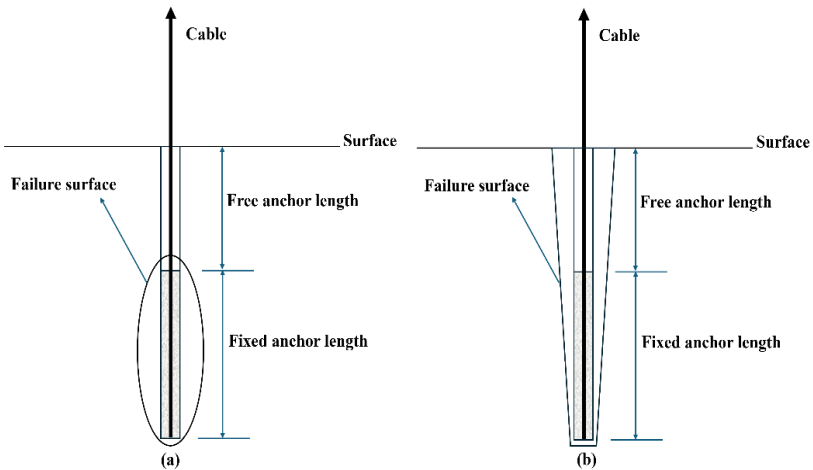


Fig. 3. Failure mode of the two different stages: (a) the proportion of fixed anchor length is less than 0.75; (b) the proportion of fixed anchor length is more than 0.75.

4 Conclusion

The following conclusions were drawn from the numerical simulation study of anchor cables with different fixed anchor length proportions at the same burial depth:

(1) As the proportion of fixed anchor length increases, there are two different damage modes of anchor cables. When the proportion of fixed anchor length is less than 0.75, the damage mode of the anchor cable is local shear damage of the surrounding rock and the damage surface is represented as an 'ellipsoid'. Conversely, when the fixed anchor length is greater than 0.75, the damage mode of the anchor cable is peripheral rock shear damage extending to the surface, and the failure surface is represented as an 'inverted cone'.

(2) The bearing capacity of the anchor cable increases with the proportion of fixed anchor length and then stabilizes when the proportion of fixed anchor length is greater than 0.75. This corresponds to the change in bearing capacity when the fixed anchor length is less than 0.75.

(3) By increasing the fixed anchor length, the bearing capacity of the anchor cable can be significantly increased.

Reference

1. Wang, S.R., Wang, Y.H., Gong, J., Wang, Z.L., Huang, Q.X., and Kong, F.L. 2020. Failure mechanism and constitutive relation for an anchorage segment of an anchor cable under pull-out loading. *Acta Mechanica*, 231(8): 3305–3317. doi:10.1007/s00707-020-02717-4.
2. Wu, A., Zhang, Y., Luo, R., Xu, D., Fan, L., Zhou, H., Wu, X., Wu, Y., and Li, Y. 2023. A Field Model Test Method of Tunnel-Type Anchorages in Rock Mass and Its Application in Railway Suspension Bridge Engineering. *Rock Mechanics and Rock Engineering*, 56(12): 8891–8906. doi:10.1007/s00603-023-03534-6.
3. Kim HK, Cho NJ. 2012 A design method to incur ductile failure of rock anchors subjected to tensile loads. *Electronic Journal of Geotechnical Engineering* 17:2737–2746.
4. Wang, K., Zhao, Y., Hu, Z., and Nie, Y. 2023. Shear Test of Pre-stressed Anchor Block and Fracture Mechanism Analysis of Anchor Cable. *Rock Mechanics and Rock Engineering*,: 589–601. doi:10.1007/s00603-022-03074-5.
5. Ren, Y., Wang, H., Wu, G., Guan, Z., and Yuan, L. 2024. Study on the anchoring performance and failure mechanism of basalt/glass hybrid fiber reinforced plastic anchors in coupled environment. *Polymer Composites*, 45(1): 946–962. doi:10.1002/pc.27828.
6. Al-Shayea, NaserA. 2024. Displacement of Rods During Pullout Failure of Rock Anchors: A Case Study. *Geotechnical and Geological Engineering*, 42(6): 5117–5141. doi:10.1007/s10706-024-02833-1.
7. Hlavička, V., and Lublőy, Ě. 2018. Concrete cone failure of bonded anchors in thermally damaged concrete. *Construction and Building Materials*, 171: 588–597. doi:10.1016/j.conbuildmat.2018.03.148.
8. Wang, D., Wu, D., He, S., Zhou, J., and Ouyang, C. 2015. Behavior of post-installed large-diameter anchors in concrete foundations. *Construction and Building Materials*,: 124–132. doi:10.1016/j.conbuildmat.2015.07.129.

9. Su, Z., Chen, J., Luo, Y., and He, X. 2021. Laboratory Model Test Research on Mechanical Characteristics of Anchor in Loess Tunnel under the Action of Pull-Out Load. *Advances in Civil Engineering*, 2021(1). doi:10.1155/2021/9997569.
10. Mohyeddin, A., Gad, E., Aria, S., and Lee, J. 2020. Effect of thread profile on tensile performance of screw anchors in non-cracked concrete. *Construction and Building Materials*, 237: 117565. doi:10.1016/j.conbuildmat.2019.117565.
11. Wen-qiang, C., and Yi-jia, L. 2022. Analytical model of bolt shear resistance considering progressive yield of surrounding material. *SN Applied Sciences*, doi:10.1007/s42452-021-04923-8.
12. Pregartner, T., and Eligehausen, R. 2007. Load Bearing Behaviour of Plastic Anchors in Cracked Concrete. *Beton- und Stahlbetonbau*, 102(S1): 22–30. doi:10.1002/best.200710101.
13. Li, Y., Gao, C., Li, Q., Wu, Q., & Meng, W. 2020. Failure Evolution Law of Reinforced Anchor System under Pullout Load Based on DIC. *Advances in Civil Engineering*, 2020(1): 1–12. doi:10.1155/2020/6640687.
14. Xu, X., and Tian, S. 2020. Load transfer mechanism and critical length of anchorage zone for anchor bolt. *PLOS ONE*, 15(1): e0227539.

Open Access This chapter is licensed under the terms of the Creative Commons Attribution-NonCommercial 4.0 International License (<http://creativecommons.org/licenses/by-nc/4.0/>), which permits any noncommercial use, sharing, adaptation, distribution and reproduction in any medium or format, as long as you give appropriate credit to the original author(s) and the source, provide a link to the Creative Commons license and indicate if changes were made.

The images or other third party material in this chapter are included in the chapter's Creative Commons license, unless indicated otherwise in a credit line to the material. If material is not included in the chapter's Creative Commons license and your intended use is not permitted by statutory regulation or exceeds the permitted use, you will need to obtain permission directly from the copyright holder.

